The X ray/EUV Selected Binary 2RE J0933+624 (FF Uma): Orbital Solution and Chromospheric Activity

M.C. Gálvez[1], D. Montes[1], M.J. Fernández-Figueroa[1],
E. De Castro [1], M. Cornide [1] ,L.W. Ramsey[2]

[1] Departamento de Astrofísica, Facultad de Físicas, Universidad Complutense de Madrid, E-28040 Madrid, Spain
[2] The Pennsylvania State University, Dep. of Astronomy and Astrophysics, 525 Davey Laboratory, PA 16802, USA

Abstract

In this contribution we present high resolution echelle spectroscopic observations taken during several observing runs (1998 - 2004) of the recently discovered, X-ray/EUV selected, active binary 2RE J0933+624 (FF UMa). We have obtained precise radial velocities by cross correlation with radial velocity standard stars for both components and we have obtained an improved orbital solution. With this information we derived other parameters and classified the system. Rotational velocity (*vsini*) have been measured too, by using the cross-correlation technique with the routine *fxcor* in IRAF. In addition, we have studied the chromosphere of this active binary system using the information provided for several optical spectroscopic features (from the Ca II H & K to Ca II IRT lines) that are formed at different heights in the chromosphere. The chromospheric contribution in these lines has been determined using the spectral subtraction technique, resulting a strong Hα emission above the continuum from both components in all the spectra as well as the emission from Ca II IRT and Ca II H & K and filled absorption lines in Hβ, Hδ and Hγ. This system shows a lithium (Li I λ6707.8) line from both components.4

Radial Velocities

Heliocentric radial velocities of both components have been determined by using the cross-correlation technique. The spectra of the program stars were cross-correlated order by order, using the routine *fxcor* in IRAF, against spectra of radial velocity standards of similar spectral types. The velocity is derived from the position of the cross-correlation peak (**Fig. 1**). As secondary emission is clearly seen in the spectra we have measured radial velocity for secondary using the wavelength difference between primary and secondary emission lines in order to get a better measured. In **Table 1** we list the obtained heliocentric radial velocities (V_{hel}) and their associated errors (σ_V) for each spectrum.

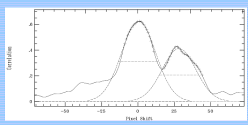

Fig. 1: Cross-correlation functions (CCFs) of the both components of the binary system, fitted with Gaussians.

Observations

The spectroscopic observations of this binary were obtained during four observing runs along 6 years:

1) 12 to 21 **January 1998** using the 2.1m *Otto Struve Telescope* at McDonald Observatory Texas (USA) with the Sandiford Cassegrain Echelle Spectrometer. During this observing run, a 1200x400 pixel CCD detector was used. The spectrograph setup was chosen to cover the Hα (6563 Å) and Ca II IRT (8498, 8542, 8662 Å) lines. The wavelength range covers from 6400 to 8800 Å in 31 orders. The reciprocal dispersion ranges from 0.06 to 0.08 Å /pixel and the spectral resolution, determined as the FWHM of the arccomparison lines, ranges from 0.13 to 0.20 Å. In one of the nights, we changed the spectrograph setup to include the He I D3 (5876 Å) and Na D1, D2 (5889.95, 5895.92 Å), with wavelength coverage of 5600-7000 Å.

2) 22 to 24 **January 2000** using the 9.2m *Hobby-Eberly Telescope* (**HET**) at McDonald Observatory Texas (USA), with the medium resolution spectrograph UFOE (Upgraded Fiber Optic Echelle). A 1200x400 pixel CCD detector was used.The wavelength range covers from 4400-9150 Å in 26 orders. The reciprocal dispersion ranges from 0.06 to 0.17 Å /pixel and the spectral resolution (FWHM) from 0.14 to 0.42 Å.

3) 22 to 25 **April 2002** using the 2.2m *Telescope* at the German Spanish Astronomical Observatory (CAHA) in Almeria (Spain), with the Fibre Optics Cassegrain Echelle Spectrometer (FOCES) (Pfeiffer et al. 1998). During this observing run, a 2048x2048 pixel 150μ Site#1d15 CCD detector was used. The spectrograph set up was chosen to cover the Hα (6563 Å) and Ca II IRT (8498, 8542, 8662 Å) lines. The wavelength range covers from 6020 to 10680 Å in 42 orders. The reciprocal dispersion ranges from 0.07 to 0.13 Å /pixel and the spectral resolution, determined as the FWHM of the arc comparison lines, ranges from 0.08 to 0.35 Å.

4) 29 March to 7 April 2004 using again the 2.2m *Telescope* at CAHA with the Site#1d15 CCD detector.
The spectrograph set up was chosen to cover the Ca H & K (3933 and 3962 Å), Ha (6563 Å) and Ca II IRT (8498, 8542, 8662 Å) lines. The wavelength range covers from 3720 to 10850 Å in 100 orders. The reciprocal dispersion ranges from 0.04 to 0.13 Å /pixel and the spectral resolution, determined as the FWHM of the arc comparison lines, ranges from 0.08 to 0.35 Å.

Chromospheric activity indicators

The chromospheric contribution in the different optical chromospheric activity indicators has been determined using the spectral subtraction technique Montes et al. (1995; 1997; 1998). The synthesized spectrum was constructed using the program STARMOD developed at Penn State (Barden 1985). The profiles of the Hα,, Hβ, Ca II H & K,Ca II IRT (λ8498, λ8542) and Li I (λ6707.8) lines are plotted in **Figs. 3, 4, 5, 6 and 7**. For each observation we have plotted the observed spectrum (solid-line) and the synthesized spectrum (dashed-line) in the left panel and the subtracted spectrum (dotted line) in the right panel except for Li line where only observed and synthesized spectrum are plotted.

Element	Value	Uncertainty	Units
P_{orb}	3.2658	0.0254	days
T_{conj}	50292.1328	0.0069	HJD
ω	39.5316	17.5390	degrees
e	0.0798	0.0220	
K_1	33.7071	0.8159	km s^{-1}
K_2	71.7446	2.0136	km s^{-1}
γ	-4.6914	0.3855	km s^{-1}
$q = M_1/M_2$	2.1285	0.0597	
a_1 sin$i$	1.5089	0.0000	10^6 km
a_2 sin$i$	3.2116	0.0901	10^6 km
a sen$i$	4.7205	0.0901	10^6 km
"	0.03155		AU
"	6.7824		$R_\odot$
$M_1 \sin^3 i$	0.2674	0.0155	$M_\odot$
$M_2 \sin^3 i$	0.1256	0.0076	$M_\odot$
f(M)	0.0128350	0.0000000	$M_\odot$

Table 2. Orbital Solution Parameters.

Obs.	MJD 2400000+	S/N (Hα)	Primary $V_{hel} \pm \sigma_V$ (km s^{-1})	Secondary $V_{hel} \pm \sigma_V$ (km s^{-1})
JEF(95)[1]	49054.591	-	23.5 ± 4.0	-35.9 ± 9.0
JEF(95)[1]	49054.634	-	26.8 ± 3.0	-30.0 ± 9.0
JEF(95)[1]	49054.675	-	22.6 ± 3.0	-45.0 ± 5.0
JEF(95)[1]	49055.378	-	20.0 ± 3.0	-53.3 ± 3.0
JEF(95)[1]	49055.423	-	19.5 ± 3.0	-47.6 ± 4.0
JEF(95)[1]	49056.425	-	-25.1 ± 5.0	48.7 ± 3.0
JEF(95)[1]	49056.486	-	-20.6 ± 4.0	58.8 ± 3.0
JEF(95)[1]	49056.543	-	-28.1 ± 4.0	57.8 ± 3.0
JEF(95)[1]	49056.600	-	-29.4 ± 4.0	57.3 ± 3.0
MCD98	50826.935	146	24.66 ± 0.92	-51.50 ± 1.75
MCD98	50827.915	203	2.74 ± 0.26	-29.26 ± 0.62
MCD98	50828.922	98	-21.99 ± 0.71	33.11 ± 1.58
MCD98	50829.929	139	24.18 ± 0.86	-55.76 ± 3.29
MCD98	50830.932	95	1.30 ± 0.25	1.30 ± 4.00
MCD98	50831.961	134	-27.26 ± 0.72	49.08 ± 1.59
MCD98	50832.958	146	15.01 ± 0.63	-30.87 ± 1.42
MCD98	50833.935	83	3.98 ± 0.51	-31.22 ± 1.72
MCD98	50834.953	77	-29.97 ± 0.78	50.15 ± 1.90
MCD98	50836.039	115	-11.94 ± 0.20	18.30 ± 0.68
HET01	51562.759	233	-6.93 ± 0.51	-6.93 ± 4.00
HET01	51566.774	263	24.55 ± 0.36	-44.29 ± 6.71
HET01	51567.812	83	-1.11 ± 0.21	-1.11 ± 4.00
HET01	51568.767	146	-33.57 ± 0.29	57.77 ± 2.70
HET01	51569.925	236	17.07 ± 0.64	-41.11 ± 2.53
FOCES02	52387.329	118	-31.06 ± 0.33	54.61 ± 1.49
FOCES02	52388.320	200	-1.58 ± 0.13	-1.58 ± 0.13
FOCES02	52389.323	140	26.82 ± 0.56	-51.75 ± 1.62
FOCES02	52390.414	146	-26.91 ± 0.63	56.14 ± 1.9
FOCES04	53096.4836	71	29.25 ± 1.34	-67.54 ± 4.67
FOCES04	53098.3186	63	-34.50 ± 1.85	62.15 ± 4.79
FOCES04	53099.3077	87	5.10 ± 1.44	-51.09 ± 3.78
FOCES04	53099.4736	74	20.32 ± 1.73	-62.52 ± 4.55
FOCES04	53099.6158	59	23.96 ± 1.49	-64.74 ± 5.94
FOCES04	53100.3048	95	23.64 ± 1.39	-56.45 ± 3.69
FOCES04	53100.4329	117	4.98 ± 1.65	-37.79 ± 3.15
FOCES04	53100.5718	80	2.38 ± 1.02	-
FOCES04	53101.3082	56	-33.20 ± 2.22	59.00± 7.71
FOCES04	53101.4374	122	-34.14 ± 2.37	61.48± 4.78
FOCES04	53101.5932	130	-35.41 ± 1.92	62.34± 5.67
FOCES04	53102.3061	117	-7.20 ± 0.84	-
FOCES04	53102.5640	93	-49.13 ± 3.98	4.84± 1.47

[1] Jefries values taken from literature

Table 1. Values of radial velocity, 9 from Jeffries et al. (1995), and 32 taken by us in four observing runs. We give here Julian date, S/N of spectral in Hα and velocities of primary and secondary component with its error.

2RE J0933+624 Orbital Solution

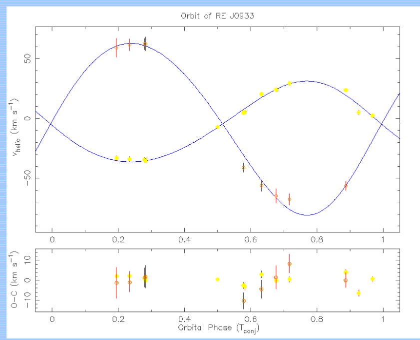

Fig. 2:Fig. 2: Radial velocity data from FOCES 2004 run and fit vs the orbital phase. Yellow solid circles represent the primary component and orange open circles represent the secondary component. The solid curves represent a minimum χ^2 fit orbit solution. In the lower panel observed minus calculated data is plotted.

Fig. 3: Hα (MacDonal 1998 and FOCES 2004)

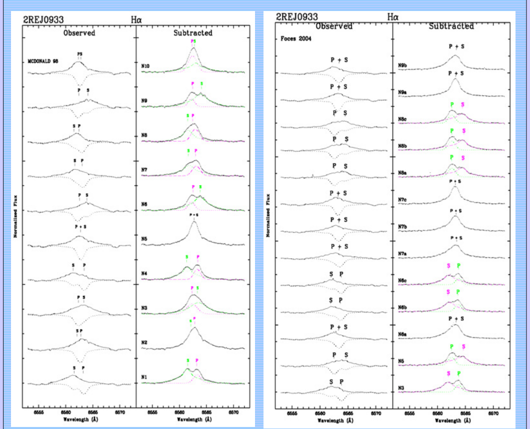

Fig. 5: CaII IRT (McDonald 1998)

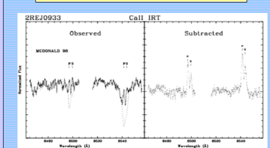

Fig. 6: Hβ (FOCES 2004)

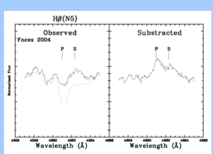

Conclusions

2RE J0933+624 (FF UMa) is an X-ray/EUV source identified as a double-lined spectroscopic binary by Jeffries et al. (1995) and Henry et al. (1995). The system consists of two rapidly rotating stars (vsin*i* = 35 km/s) classified as G5 by Jeffries et al. (1995) and as K0 by Henry et al. (2000). Both authors noted that the primary should be a subgiant, while the secondary is still on the main sequence in agreement with relative contribution of the photospheric lines in our spectra.
We have found that the best fitting for spectral subtraction be using a **KIV** primary component with a 70% of contribution to continuum and a **K0V** secondary with the 30%.

Jeffries et al. (1995) give a preliminary orbit for this system with a eccentricity *e*=0.18 and an orbital period of 3.28 days similar to the photometric period reported by Henry et al. (2000) indicating nearly synchronous rotation. The radial velocities determined by us in FOCES 2004 observing run (**Table 1**) also indicate a eccentric orbit with e ≈ 0.08 and an orbital period of 3.2658 days.
From the orbit solution parameters (**Table 2**) (q=2.1285) we can deduce, assuming that secondary component is a K0V, that the mass of the primary is around 1.58 solar masses, in concordance with a K subgiant primary component.

Both components exhibit Hα emission above the continuum (**Fig. 3**) in all our spectra. The strongest emission correspond to the secondary component, which also show very broad wings. The excess emission of this component has been fitted using a three Gaussians fit, one for primary component and two (a narrow and wide component) for secondary. The last one show how the wide component move left and right respect narrow one indicating changes in the microflaring activity.

Emission in the Ca II IRT lines superimposed to the corresponding absorption lines (**Fig. 2 and 5**), are also detected from both components , as well as in the Ca II H & K lines (**Fig. 3**) and the filling-in of the rest Balmer lines (see Hβ in **Fig. 6**).

Fig. 4: CaII IRT and Ca II H&K (FOCES 2004)

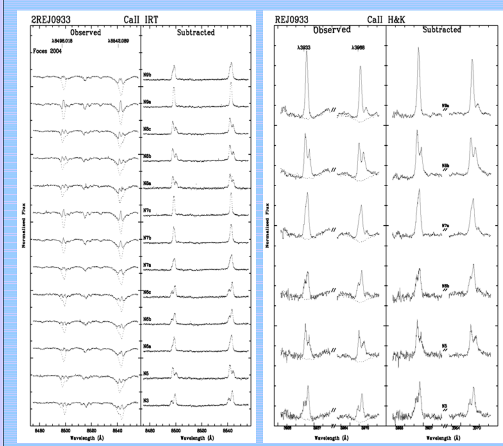

Fig. 7: Li I (FOCES 2004)

We also can see the absorption of Li (λ6707.8) from both component in (Fig. 7). The EW measured in the observed spectrum is 58 mÅ for the primary component and 65 mÅ for the secondary.